

SPECTRAL PROPERTIES OF SINGLE CRYSTALS OF SYNTHETIC DIAMOND

G. A. Gusakov,^a M. P. Samtsov,^{a*} E. S. Voropai,^b V. S. Solov'ev,^a
and A. N. Demenshenok^a

UDC 535.33.36

The half-width of the spectrum of Raman scattering (RS) of the first order of a diamond single crystal grown in a nickel-free system containing nitrogen getters is identical to all growth sectors ($1.69 \pm 0.02 \text{ cm}^{-1}$). The sectorial inhomogeneity is not reflected in the transmission spectra and birefringence of this crystal. The nitrogen concentration is $4 \cdot 10^{17} \text{ cm}^{-3}$. For different growth sectors of the diamond crystal grown in the Ni-Fe-C system, the half-width of the Raman line varies from 1.74 to 2.08 cm^{-1} , differences in the transmission spectra and birefringence are observed, and photoluminescence is revealed. The concentration of nitrogen in the growth sectors {001} is $1.6 \cdot 10^{19} \text{ cm}^{-3}$, the content of nickel is estimated to be at a level of 10^{19} cm^{-3} , and the content of nitrogen in the $\{\bar{1}11\}$ sectors is $4 \cdot 10^{19} \text{ cm}^{-3}$.

Keywords: *Raman scattering, synthetic diamond single crystals, transmission, birefringence, impurities.*

The past decade has been characterized by significant advances in the technology of the synthesis of diamond: we have succeeded in coming close to the possibility of growing large single crystals of instrumental quality [1, 2]. The introduction into industry of the synthesis of high-quality crystals with a controlled impurity composition and uniform distribution of doping agents and background impurities offers the future prospect of solving the problem of a shortage of natural diamond raw material in optics and electronics.

Synthetic diamonds are grown in high-pressure "belt"-type apparatuses based on high-power hydraulic presses [3] or apparatuses of the "split sphere" type without presses [4]. The structure and impurity composition of the synthetic diamond single crystals obtained in a "belt"-type high-pressure apparatus have been studied rather thoroughly [3–8], unlike the crystals obtained in a high-pressure apparatus of the second type. Along with the optical and gemological properties which are common to all synthetic diamonds, the specimens grown in the apparatuses of different types can have a number of essential differences [9, 10].

The purpose of the present work is to study the birefringence, absorption, and RS spectra of synthetic diamonds grown using various systems of metals-solvents in a "split sphere"-type high-pressure apparatus.

Experimental Objects and Procedures. The only technique allowing large crystals of diamond to be grown is the temperature-gradient method [11, 12]. Crystals were grown under the conditions of thermodynamic stability of diamond ($P = 5.2\text{--}6.0 \text{ GPa}$, $T = 1400\text{--}1600^\circ\text{C}$) by recrystallizing, onto a diamond seed, a source carbon dissolved in a molten metal. The crystals were synthesized at the Adamas Research and Production Enterprise. The pressure in the high-pressure apparatus was calibrated in a cold state against phase

*To whom correspondence should be addressed.

^aA. N. Sevchenko Institute of Applied Physical Problems, 7 Kurchatov Str., Minsk, 220064, Belarus; e-mail: samtsov@pfp.bs.uibel.by; ^bBelarusian State University, Minsk, Belarus. Translated from *Zhurnal Prikladnoi Spektroskopii*, Vol. 68, No. 5, pp. 612–616, September–October, 2001. Original article submitted April 21, 2001.

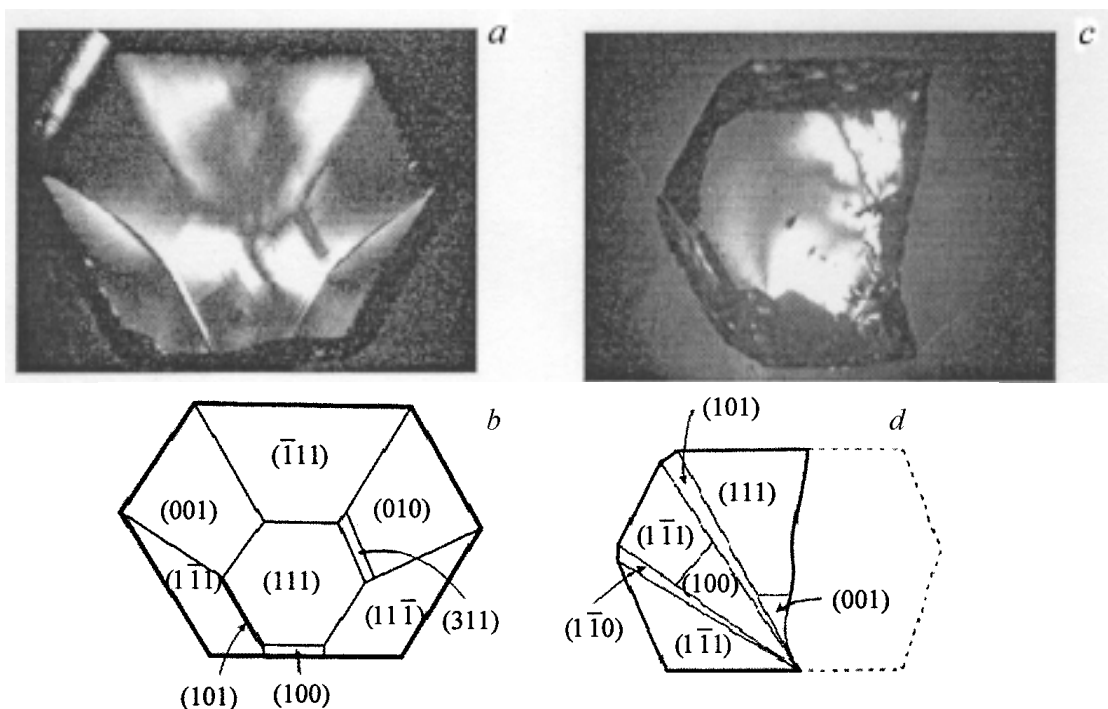


Fig. 1. Photographs of plates 1 (a) and 2 (c) in crossed polarizers; the scheme of sectorial structure of plates 1 (b) and 2 (d).

transitions in chalcogenides. The temperature in the reaction zone was controlled by a TPP thermocouple, whose junction was positioned near the carbon source. Absolute temperatures were determined allowing for pressure [13].

Two synthetic diamond single crystals with a mass of 0.7–0.8 ct were the objects of study. Crystal 1 was grown in the Ni–Fe–C system at $P = 5.4$ GPa and $T = 1450^\circ\text{C}$. The seed was oriented to the $\{111\}$ plane. In shape the crystal is a cuboidal octahedron truncated along the L_3 symmetry axis with minor faces $\{110\}$ and $\{113\}$. There were no inclusions that would be visible to the unaided eye in the bulk of the crystal. Crystal 2 was grown in the Fe–Al–C system at $P = 5.5$ GPa and $T = 1500^\circ\text{C}$; aluminum had been introduced as a gettering additive for nitrogen fixation [12]. The seed was oriented to the $\{001\}$ plane. In shape the crystal is a cuboidal octahedron truncated along the L_4 symmetry axis with minor faces $\{110\}$ and $\{113\}$. Two large (up to 1 mm) and some fine inclusions of the metal-solvent were observed in the near-seed region (lower part of the crystal). Plane-parallel plates with a thickness of about 1 mm (hereinafter plates 1 and 2) were cut out of these crystals and their properties were studied. During machining (polishing), plate 2 split into two parts.

The birefringence in the plates was studied with the aid of an R-113 polarization microscope coupled with a videocamera and a computer. Transmission spectra were recorded on a two-beam Specord M40 or one-beam Solar PV1251a spectrophotometer. Sections of the specimens for study of transmission were isolated by a 0.5-mm-hole diaphragm.

The Raman spectra were recorded at room temperature with the aid of a Spex 1403 Raman spectrometer with a system of thermostabilization of a monochromator. In the spectral region of about 500 nm the resolution achieved with this spectrometer is 0.15 cm^{-1} . The spectra were recorded by a backscattering scheme. The excitation was provided by radiation of an Ar^+ laser (488 or 514.5 nm). The radiation power on a specimen was 0.3–0.4 W, the exciting beam was about 10 μm in diameter, and the spectral half-width of

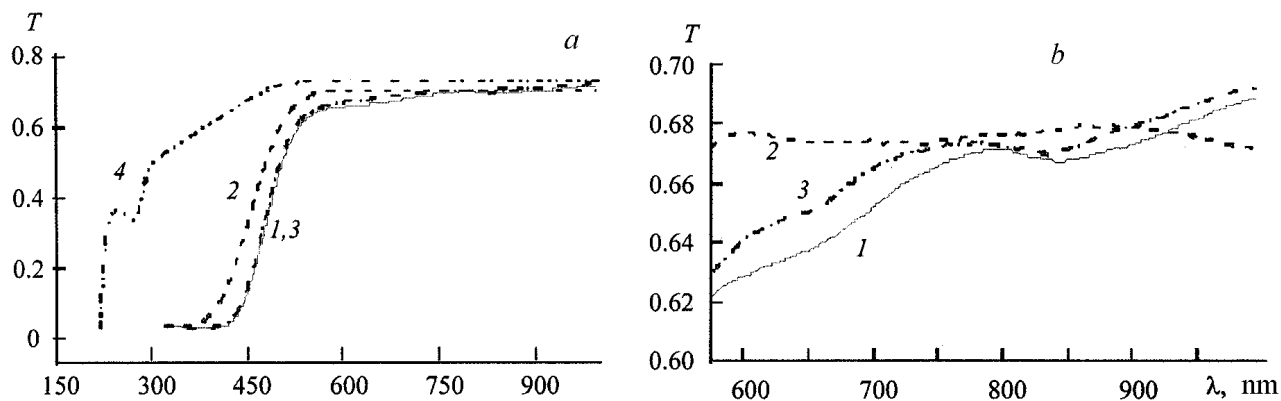


Fig. 2. Transmission spectra of the growth sector $\{\bar{1}11\}$ of plate 1 (1), the sector $\{001\}$ of plate 1 (2), the sector $\{111\}$ of plates 1 (3) and 2 (4).

the slits of the spectrometer was 0.3 cm^{-1} . The half-width and the position of the peak of the RS band of diamond were determined by employing approximation of experimental data by the Lorentz function.

Results and Discussion. Patterns of the birefringence and schemes of the sectorial structure of the specimens under investigation are presented in Fig. 1. The analysis of the patterns obtained shows that in the growth sectors $\{111\}$ of plate 1 excess internal stresses are located and, conversely, they are not detected in the sectors $\{001\}$. This inhomogeneity in the characteristics of the crystal is associated with nonuniform trapping of impurity atoms by various growth sectors [14].

As is seen from the transmission spectra of crystal 1 (Fig. 2), considerable absorption in the short-wave region ($\lambda < 550 \text{ nm}$) is characteristic of the basic growth sectors. For the growth sector $\{\bar{1}11\}$ practically total absorption is observed when $\lambda \leq 420 \text{ nm}$, and for the sector $\{001\}$ this is the case when $\lambda \leq 350 \text{ nm}$ (Fig. 2a). In going to the near IR region, there is a monotonic reduction in transmission and weak wide absorption bands with peaks at about 650 and 850 nm for the growth sector $\{\bar{1}11\}$ (Fig. 2b). For the growth sector $\{001\}$, there are no information peaks in this region.

The presence of absorption in diamonds for $\lambda < 550 \text{ nm}$ is usually associated with the presence of single atoms of nitrogen in a substituting position (C defect) in their lattice [15]. In [15], the following relationship was established between the absorption coefficient at a wavelength of $\lambda = 477 \text{ nm}$ (α_{477}) and the concentration of the C defects (N_C):

$$N_C = 2.8 \cdot 10^{18} \alpha_{477}.$$

For crystal 1, the concentration of C defects in the growth sectors $\{001\}$ and $\{111\}$ was $1.6 \cdot 10^{19}$ and $3.9 \cdot 10^{19} \text{ cm}^{-3}$, respectively.

The wide absorption bands at 650 and 850 nm can be attributed to the presence of the atoms of nickel in the diamond lattice [16–18]. The presence of this metal in the crystals of diamond is usually recorded in the absorption spectra at the liquid nitrogen temperature. The appearance of these bands at room temperature indicates a relatively high concentration of the nickel impurity in the growth sector $\{\bar{1}11\}$. The monotonic increase of absorption in going to the near IR band, which is observed for the growth sector $\{001\}$, can be due to the broken bonds on dislocations [19].

In contrast to plate 1, we failed to find a sectorial structure in the birefringence patterns of specimen 2. The excess internal stresses are associated with the inclusions of the metal-solvent. The transmission spectrum in the UV and visible ranges for specimen 2 is given in Fig. 2a. In the 225-nm region, an edge of the

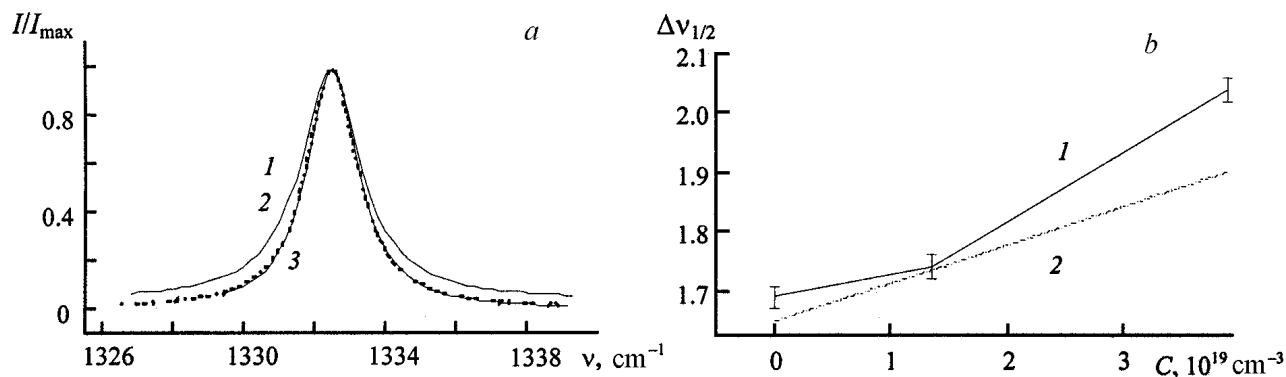


Fig. 3. RS spectrum of plate 1 of the growth sector $\{\bar{1}11\}$ with excitation at $\lambda = 488$ (1) and 514.5 nm (2); the spectrum of second order for samples 1 and 2 (3).

true fundamental absorption of diamond is observed in the spectrum. The absorption band with a peak in the 275-nm region is caused by the presence of C defects in the lattice of the diamond [15]. Other absorption bands were not observed in the UV and visible ranges. According to the relationship obtained in [15, 20], one can determine the total concentration of nitrogen in a crystal from the known absorption coefficient:

$$N_C = 1 \cdot 10^{17} \alpha_{275}.$$

For crystal 2, the concentration of nitrogen was $4 \cdot 10^{17} \text{cm}^{-3}$. According to the classification adopted in [15], this specimen closely resembles the IIa type natural crystals.

The RS spectrum of the crystals under investigation consists of a narrow line of the first order spectrum and of a substantially less intense and wide band of the second order (Fig. 3). The RS spectra of each of the specimens under investigation were recorded at several points of the plates with allowance for the sectorial structure of the crystals. The largest changes were observed in the region of the first-order spectrum. Accordingly, the results of the analysis of the RS spectra for a rather narrow frequency band of 1320–1340 cm^{-1} are presented in this work (Fig. 4). It should be noted that the spectra were recorded from one point of the specimen in five scannings; the error of reproducibility of the peak position and of the half-width of the RS band of first order in this range did not exceed 0.1cm^{-1} and 0.02cm^{-1} , respectively.

The position of the peak of the RS band of the first order in the 1332.5-cm^{-1} region for different growth sectors of both plates remained constant within the limits of the measuring accuracy. At the same time, the half-width of this line underwent appreciable changes (Fig. 4a). The half-width exceeded 2cm^{-1} and was less than 1.8cm^{-1} for the $\{\bar{1}11\}$ and $\{001\}$ sectors of plate 1, respectively. The change in the half-width of the RS band was also observed within each of the growth sectors of plate 1. The half-widths changed from $1.74 \pm 0.02 \text{cm}^{-1}$ to $1.78 \pm 0.02 \text{cm}^{-1}$ and from $2.00 \pm 0.02 \text{cm}^{-1}$ to $2.08 \pm 0.02 \text{cm}^{-1}$ for the $\{001\}$ and $\{\bar{1}11\}$ sectors, respectively. These data are indicative of a considerable difference in the impurity concentrations in these sectors and are in agreement with the results obtained from the transmission spectra. The fluctuations of the half-width within the growth sector can be interpreted as nonuniform distribution of the impurities. The more considerable change of the half-width in the $\{\bar{1}11\}$ growth sectors points to the larger inhomogeneity in the distribution of the impurity in these sectors in comparison with the $\{001\}$ ones. It should also be noted that for the growth sectors $\{\bar{1}11\}$ considerable background luminescence is detected on exciting by the radiation with $\lambda = 488 \text{nm}$ (Fig. 3), whereas for $\lambda = 514.5 \text{nm}$ its intensity is two orders of magnitude lower. For the growth sectors $\{001\}$, in excitation with $\lambda = 488 \text{nm}$, the luminescence intensity

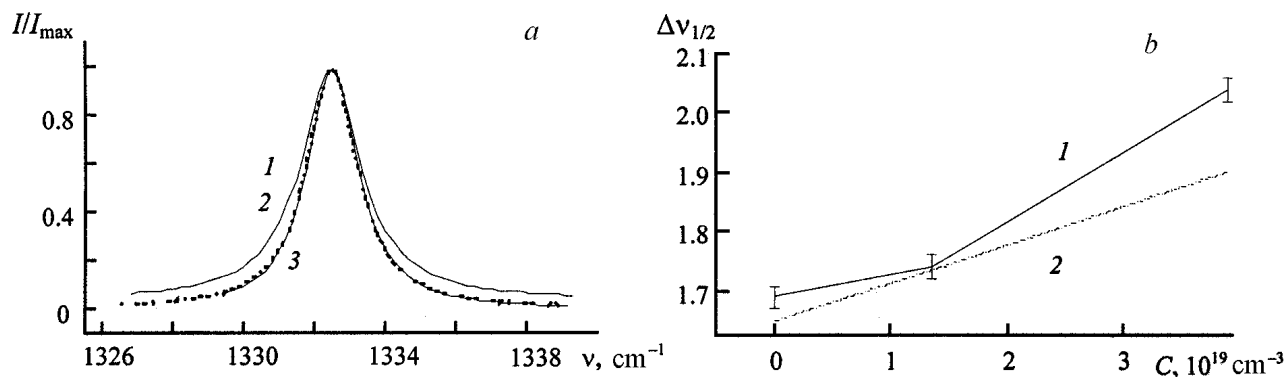


Fig. 4. RS spectra of the first order (a) of sample 1 of the growth sectors $\{\bar{1}11\}$ (1) and $\{001\}$ (2) and of sample 2 (3); the dependence of the half-width of the Raman line of diamond on the nitrogen concentration (b): experimental (1) and calculated (2) data.

is an order of magnitude lower than for the sectors $\{\bar{1}11\}$ and it is practically absent in excitation with $\lambda = 514.5$ nm. In scanning by an exciting beam ($\lambda = 488$ nm) across the growth sector $\{\bar{1}11\}$, the intensity of photoluminescence changed from point to point by more than an order of magnitude, thus indicating the inhomogeneous distribution of the luminescence centers. At the same time, we failed to find any correlation between the half-width of the RS band and the luminescence intensity of the crystal. Most likely, the concentration of the centers causing photoluminescence is insufficiently high for their presence to be revealed in the RS spectra.

The least half-width of the Raman line of $1.69 \pm 0.02 \text{ cm}^{-1}$ was fixed for plate 2 (Fig. 4). The line half-width for this crystal did not depend on the position of the point from which the spectra were recorded. This value is close to 1.65 cm^{-1} , which was obtained in [16] for the most perfect natural diamond of the type IIb. The slight broadening of the Raman line appears to be due to the presence of inclusions of the metal-solvent in the crystal. There was no photoluminescence in this crystal.

The increase in the half-width of the Raman line is proportional to the elastic deformation arising in the crystalline lattice of diamond [21] due to the difference in the covalent radii of the matrix and impurity atoms. The relative deformation of the crystal is related to the atomic fraction of the impurity by the following relation [21]:

$$\varepsilon = [1 + f(\Gamma^3 - 1)]^{1/3} - 1, \quad (1)$$

where f is the atomic fraction of the impurity and Γ is the ratio of the covalent radii of the atoms of the dissolved impurity and carbon. In the case of nitrogen atoms located in the sites of the diamond lattice (C defects), $\Gamma = 0.922$.

On the basis of the results obtained for the growth sectors $\{001\}$ of crystal 1 (low level of internal stresses and photoluminescence, absence of light absorption for $\lambda > 500$ nm), it is possible to assume the presence only of nitrogen impurity in the form of C defects. The mean half-width of the Raman line for these sectors differs by 0.11 cm^{-1} in comparison with the most perfect natural diamond of type IIb. If this difference in the half-width is considered to be due exclusively to the presence of nitrogen, then, using expression (1), it is possible to plot the dependence of the half-width of the Raman line on the concentration of C defects in single crystals of diamond (Fig. 4b). Owing to the presence of C defects, the half-width should be 1.92 cm^{-1} for the growth sectors $\{\bar{1}11\}$ of crystal 1 (Fig. 4b). The higher half-width (up to 2.08 cm^{-1}) ob-

tained for this region can be attributable to the presence of nickel in the growth sectors $\{\bar{1}11\}$ of crystal 1. Assuming that all the atoms of nickel in the diamond lattice are in the substituting state, it is possible to estimate the concentration of this impurity from relationship (1). Accounting for the partial compensation of the internal stresses created by the nitrogen and nickel atoms (in the case of nickel, $\Gamma = 1.61$), a half-width of 2.04 cm^{-1} corresponds to the concentration of nickel of about $7 \cdot 10^{18} \text{ cm}^{-3}$. This value correlates with the data in [22].

The analysis of the results obtained and their comparison with those given in [5–8] show that the investigated diamond crystals grown in the high-pressure apparatus of the "split sphere" type are close in the impurity composition and the character of the impurity distribution to the crystals obtained in a high-pressure apparatus of the "belt" type in the De Beers laboratories. One should note, however, the less complex sectorial structure of the crystals studied in comparison with those described in [6, 7].

The following conclusions can be drawn on the basis of the analysis of the RS and absorption spectra and the birefringence of the diamond crystals grown in the high-pressure apparatus of the "split sphere" type using various systems of metals-solvents. The crystals grown in the nickel-free systems containing nitrogen getters have a more perfect crystal structure. They do not display sectorial inhomogeneity. In their optical characteristics (transparency in the UV and visible ranges of the spectrum, the half-width of the Raman line) they closely resemble the most perfect natural diamonds. The crystals grown in the Ni–Fe–C system display considerable sectorial inhomogeneity of the impurity distribution. The growth sector $\{\bar{1}11\}$ contains 2.5 times more nitrogen and several times more nickel than the sector $\{100\}$. The nitrogen concentration in the growth sector $\{\bar{1}11\}$ reaches $4 \cdot 10^{19} \text{ cm}^{-3}$, and the nickel content is estimated at a level of 10^{19} cm^{-3} . The sectorial distribution of the impurity leads to the appearance of excess internal stresses and to substantial inhomogeneity of the optical characteristics of the crystal.

The authors express their gratitude to the administration and staff of the Adamas Research and Production Enterprise (Atolino, Minsk District, Belarus) for their help in carrying out the experiments on growing single crystals of synthetic diamond.

This work was supported by the Belarusian Republic Foundation for Fundamental Research, grant No. F00-206.

REFERENCES

1. Y. Shuji, *J. Soc. Mater. Sci. Jpn.*, **42**, No. 476, 588–593 (1993).
2. H. Sumiya and S. Satoh, *Diam. Rel. Mater.*, **5**, 1359–1365 (1996).
3. H. T. Hall, *Rev. Sci. Instr.*, **31**, No. 2, 125–131 (1960).
4. Yu. N. Pal'yanov, I. Yu. Malinovskii, Yu. M. Borzdov, et al., *Dokl. Akad. Nauk SSSR*, **315**, No. 5, 1221–1224 (1990).
5. F. C. Frank, A. R. Lang, D. J. F. Evans, et al., *J. Cryst. Growth*, **100**, 354–376 (1990).
6. R. C. Burns, Cvetkovic, C. N. Dodge, et al., *J. Cryst. Growth*, **104**, 257–279 (1990).
7. W. Wierzchowski, M. Moore, A. P. W. Makepeace, et al., *J. Cryst. Growth*, **114**, 209–227 (1991).
8. H. Sumiya, N. Toda, Y. Nishibayashi, et al., *J. Cryst. Growth*, **178**, 485–494 (1997).
9. V. D. Antsygin, Yu. M. Borzdov, V. A. Gusev, et al., *Avtometriya*, **5**, 10–15 (1995).
10. J. E. Shigley, E. Fritsch, J. I. Koivula, et al., *Gems Gemology*, **29**, No. 4, 228–248 (1993).
11. H. M. Strong and R. E. Hanneman, *J. Chem. Phys.*, **46**, No. 9, 3668–3676 (1967).
12. H. M. Strong and R. M. Chrenko, *J. Phys. Chem.*, **75**, No. 12, 1838–1843 (1971).
13. F. P. Bundy, *J. Appl. Phys.*, **32**, 483–494 (1961).
14. A. S. Varshavskii, *Anomalous Birefringence and Internal Morphology of Diamond* [in Russian], Moscow (1968).

15. G. B. Bokii, G. N. Bezrukov, Yu. A. Klyuev, et al., *Natural and Synthetic Diamonds* [in Russian], Moscow (1984).
16. S. A. Solin and A. E. Ramdas, *Phys. Rev.*, **B1**, No. 4, 1687–1699 (1970).
17. S. C. Lawson and H. Kanda, *Diam. Rel. Mater.*, **2**, 130–135 (1993).
18. A. T. Collins, H. Kanda, and R. C. Burus, *Phil. Mag.*, **61**, No. 5, 797–810 (1990).
19. V. B. Kvaskov (ed.), *Natural Diamonds of Russia* [in Russian], Moscow (1997).
20. R. M. Chrenko, H. M. Strong, and R. E. Tuft, *Phil. Mag.*, **23**, 313–318 (1971).
21. J. R. Carruthers, R. B. Hoffman, and J. D. Ashner, *J. Appl. Phys.*, **34**, 3389–3392 (1963).
22. M. I. Samoilovich, G. N. Bezrukov, and V. P. Butuzov, *Pis'ma Zh. Éksp. Teor. Fiz.*, **14**, No. 10, 551–553 (1971).